Liquid Crystals
Publication details, including instructions for authors and subscription information:
http://www.informaworld.com/smpp/title~content=t713926090

Effect of chiral isosorbide groups on mesomorphic properties of side-chain liquid-crystalline polysiloxanes

Heng-Da Gu[a]; Li Chen[a]; Jing-Xi Yan[a]
[a] School of Applied Chemistry, Shenyang Institute of Chemical Technology, Shenyang, People's Republic of China

First published on: 08 October 2009

To cite this Article Gu, Heng-Da , Chen, Li and Yan, Jing-Xi(2009) 'Effect of chiral isosorbide groups on mesomorphic properties of side-chain liquid-crystalline polysiloxanes', Liquid Crystals, 36: 12, 1319 — 1327, First published on: 08 October 2009 (iFirst)
To link to this Article: DOI: 10.1080/02678290903220980
URL: http://dx.doi.org/10.1080/02678290903220980

Liquid Crystals,
Vol. 36, No. 12, December 2009, 1319–1327

Taylor & Francis
Taylor & Francis Group

Effect of chiral isosorbide groups on mesomorphic properties of side-chain liquid-crystalline polysiloxanes

Heng-Da Gu*, Li Chen and Jing-Xi Yan

School of Applied Chemistry, Shenyang Institute of Chemical Technology, Shenyang 110142, People's Republic of China

(Received 6 May 2009; final form 30 July 2009)

Chiral side-chain liquid-crystalline (LC) polysiloxanes containing isosorbide groups were graft copolymerised with poly(methylhydrogeno)siloxane, a chiral LC monomer 6-(4-methoxy-benzoyloxy)-hexahydro-furo[3,2-*b*]furan-3-yl 4'-(4-undec-10-enoyloxy-benzoyloxy)-biphenyl-4-yl adipate and a nematic LC monomer 4'-(4-methoxy-benzoyloxy)-biphenyl-4-yl 4-(2-undec-10-enoyloxy-ethoxy)-benzoate. The chemical structures and LC properties of the monomers and polymers were characterised by use of various experimental techniques including Fourier transform infrared spectroscopy (FTIR), ^{1}H-nuclear magnetic resonance (NMR), element analyses (EA), differential scanning calorimetry (DSC), polarised optical microscopy (POM) and X-ray diffraction (XRD). All the chiral LC polymers showed LC properties with very wide mesophase temperature ranges and the chiral component in the LC polymer systems lead to the appearance of a cholesteric phase. The polymers bearing most chiral LC monomer component showed smectic phases by reason of regular structures in the polymer systems. With the increase of another nematic LC monomer in the polymers, the regular polymer structures were destroyed because of different chemical structures between the two kinds of LC monomers, leading to the disappearance of the smectic arrangement.

Keywords: liquid-crystalline polymers; polysiloxanes; chiral; phase behaviour

1. Introduction

Side-chain liquid-crystalline polymers (LCPs) combine the electro-optical properties of low molecular weight liquid crystals with the mechanical properties and easy processing of polymers. A focus of interest in the synthesis of LCPs is the preparation of chiral LCPs. Chirality has become one of the most important and complex topics in liquid crystal research. This is mainly due to the fact that molecular asymmetry imparts form chirality to the liquid crystalline (LC) phases and leads to possible new technical applications for chiral LCPs (*1–7*).

Chiral LCPs may exhibit a marvellous variety of LC phases, including the chiral smectic C* (S_C*) phase, the cholesteric (Ch) phase, and the blue phases (BP*) (*8–12*). Being a chirality-dependent quantity, the Ch twist can be right- or left-handed, depending on the configuration of the chiral elements within the molecule. For S_C* phases, there is an acute angle between the molecular axis and the helical axis. BP* are generally frustrated defect phases between the isotropic phase and Ch or smectic phases of highly chiral mesogens. Chiral smectic LCPs composed of chiral mesogens have attracted both industrial and scientific interest because their additional properties, such as piezoelectricity, ferroelectricity and pyroelectricity, result from the symmetry breaking brought about by molecular chirality (*13–16*). Side-chain ferroelectric and piezoelectric LCPs have been investigated extensively because they combine the properties of ferroelectric and piezoelectric liquid crystals, showing better mechanical properties and ease of processing compared with small-molecule liquid crystals. Ch liquid crystals are well known for their unique optical properties arising from their helicoidal supramolecular structures characterised by a pitch (*P*) and handedness. A Ch liquid crystal may selectively reflect left- or right-handed circularly polarised light with the handedness determined by its twist sense, and the wavelength of reflection is related to its pitch (*P*). Ch polymers have interesting optical properties that are useful for optically active films, coatings, or pigments (*17–19*).

Because chiral LCPs exhibiting different LC phases result in different industrial applications, it is important to study the mesomorphic properties of chiral LCPs bearing a definite chiral group. In the present study, we prepared a series of polysiloxane-based side-chain LCPs containing isosorbide groups.

2. Experimental

2.1 Materials

10-Undecylenoic acid, biphenyl-4,4'-diol, p-hydroxybenzoic acid, 4-methoxy-benzoic acid, adipic acid, isosorbide, hexachloroplatinic acid hydrate and poly(methylhydrogeno)siloxane (PMHS) (M_n = 600–800) were obtained from the Jilin Chemical Industry Company and used without any further

*Corresponding author. Email: hengdagu@163.com

ISSN 0267-8292 print/ISSN 1366-5855 online

DOI: 10.1080/02678290903220980
http://www.informaworld.com

purification. Pyridine, thionyl chloride, chlorethyl alcohol, toluene, ethanol, chloroform, tetrahydrofuran (THF) and methanol were purchased from the Shenyang Chemical Co. Pyridine was purified by distillation over KOH and NaH before using.

2.2 Measurements

Fourier transform infrared spectroscopy (FTIR) spectra of the synthesised polymers and monomers in a solid state were obtained by the KBr method performed on PerkinElmer instruments Spectrum One Spectrometer (PerkinElmer, Foster City, CA). ^{1}H-nuclear magnetic resonance (NMR) (300 MHz) spectra were obtained with a Varian Gemini 300 NMR Spectrometer (Varian Associates, Palo Alto, CA) with Fourier transform, with dimethyl sulfoxide-d_6 (DMSO-d_6) or $CDCl_3$ as a solvent and tetramethylsilane (TMS) as an internal standard. The element analyses (EA) were carried out using an Elementar Vario EL III (Elementar, Germany). The thermal properties were characterised by use of a NETZSCH instruments DSC 204 and a TG 209 (Netzsch, Wittelsbacherstr, Germany) at a heating rate of 10°C min^{-1} under a nitrogen atmosphere. The phase transition temperatures were collected during the second heating and the first cooling scans. A visual observation of LC transitions and optical textures under cross-polarised light was made with a Leica DMRX (Leica, Wetzlar, Germany) polarised optical microscope equipped with a Linkam THMSE-600 (Linkam, Surrey, England) hot stage. X-ray diffraction (XRD) of the samples was performed using Cu Kα(λ = 1.542 Å) radiation monochromatised with a Rigaku DMAX-3A X-ray diffractometer. The measurement of optical rotation (α) was carried out with a PerkinElmer instrument Model 341 Polarimeter using a sodium light source (λ = 589 nm).

2.3 Synthesis of monomers and polymers

2.3.1 Synthesis of 6-(4-methoxy-benzoyloxy)-hexahydro-furo[3,2-b]furan-3-yl 4'-(4-undec-10-enoyloxy-benzoyloxy)-biphenyl-4-yl adipate (M1)

Scheme 1 shows the synthesis route of the chiral LC monomer **M1** bearing the isosorbide group. 4-Undec-10-enoyloxy-benzoyl chloride (**1**) was synthesised according to a reported procedure (*20*). Biphenyl-4,4'-diol (46.5 g, 0.35 mol) and 8 mL pyridine were dissolved in 150 mL dry THF. It was added dropwise with a solution of **1** (0.10 mol) that was dissolved in 15 mL THF. The reaction mixture was stirred at 65°C for 10 h. After cooling to room temperature, the mixture was poured into 200 mL cold water and acidified with 6 N sulfuric acid. The precipitates were isolated by filtration and dried in a vacuum oven. Recrystallisation in alcohol and acetone resulted in white crystals of 4'-(4-undec-10-enoyloxy-benzoyloxy)-biphenyl-4-ol (**2**). Yield: 65%. m.p.: 174°C. Infrared (IR) (KBr, cm^{-1}): 3412 (–OH), 3055, 2921, 2849 (–CH_2–, CH_2= and =CH), 1754, 1714 (C=O), 1601, 1505 (Ar), 1272 (C–O–C). ^{1}H-NMR ($CDCl_3$, δ, ppm): 1.30–1.75 [m, 12H, –(C<u>H</u>$_2$)$_6$–]; 1.95–2.10 (m, 2H, =CHC<u>H</u>$_2$–); 2.25–2.65 [m, 2H, –(CH$_2$)$_6$C<u>H</u>$_2$COO–]; 5.05–5.18 (m, 2H, C<u>H</u>$_2$=CH-); 5.73–5.80 (m, 1H, CH$_2$=C<u>H</u>–); 6.01–6.12 (s, 1H, –O<u>H</u>), 6.84-7.95 (m, 12H, Ar-<u>H</u>).

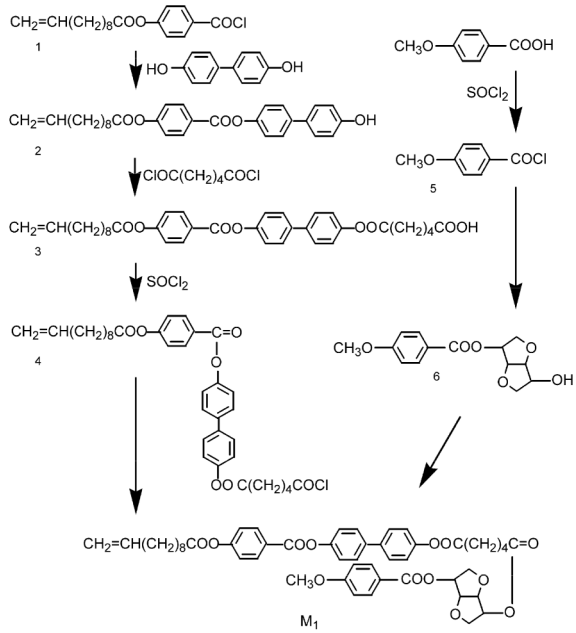

Scheme 1. Synthesis routes of 6-(4-methoxy-benzoyloxy)-hexahydro-furo[3,2-*b*]furan-3-yl 4'-(4-undec-10-enoyloxy-benzoyloxy)-biphenyl-4-yl adipate (**M1**).

Adipoyl chloride (0.5 mol) was dissolved in 15 mL THF, which was prepared by adipoyl acid and excess thionyl chloride via the normal method. It was added dropwise with 50 mL dry THF solution containing intermediate **2** (34.2 g, 0.10 mol) and 1 mL pyridine. The reaction mixture was stirred at 65°C for 10 h. After cooling to room temperature, the mixture was poured into 250 mL cold water and acidified with 6 N sulfuric acid. The precipitates were isolated by filtration, washed with hot water, recrystallised in alcohol and dried in a vacuum oven to obtain white crystals of 5-(4'-(4-undec-10-enoyloxy-benzoyloxy)-biphenyl-4-yl)-oxycarbonyl pentanoic acid (**3**). Yield: 71%. m.p.: 148°C. IR (KBr, cm^{-1}): 2923, 2850 (–CH_2–, CH_2= and =CH), 2671–2556 (–OH in –COOH), 1747, 1715, 1684 (C=O), 1602, 1509 (Ar), 1271 (C–O–C). ^{1}H-NMR ($CDCl_3$, δ, ppm): 1.29–1.96

[m, 16H, –(C<u>H</u>$_2$)$_6$– and –(C<u>H</u>$_2$)$_2$–]; 2.01–2.16 (m, 2H, =CHC<u>H</u>$_2$–); 2.35–2.84 [m, 6H, –(CH$_2$)$_6$C<u>H</u>$_2$COO– and –OOCC<u>H</u>$_2$(CH$_2$)$_2$C*H*$_2$COO–]; 5.01–5.12 (m, 2H, C<u>H</u>$_2$=CH–); 5.75–5.92 (m, 1H, CH$_2$=C<u>H</u>–); 7.02–8.05 (m, 12H, Ar-<u>H</u>); 10.02 (S, 1H, -COO<u>H</u>).

The intermediate **3** (23.5 g, 0.050 mol), 80 mL thionyl chloride and 1.0 mL of pyridine were added into a round flask equipped with an absorption instrument of hydrogen chloride. The mixture was stirred at room temperature for 3 h, then heated to 60°C and kept for 5 h in a water bath to ensure that the reaction finished. The excess thionyl chloride was distilled under reduced pressure. Then 100 mL cold THF was added to the residue at 20°C to obtain a THF solution of (5-(4'-(4-undec-10-enoyloxy-benzoyloxy)-biphenyl-4-yl)-oxycarbonyl)-pentanoyl chloride (**4**).

Isosorbide (219.0 g, 1.50 mol) and 50 mL dry pyridine were dissolved in 50 mL dry THF. It was added dropwise with 4-methoxy-benzoyl chloride (**5**, 51.0 g, 0.35 mol) prepared by 4-methoxy-benzoic acid and excess thionyl chloride via the normal method. The reaction mixture was stirred at 60°C for 36 h, and then some solvent was distilled out. After cooling to room temperature, the residue mixture was poured into 500 mL cold water. The yellow precipitates were washed with hot water and alcohol, isolated by filtration, recrystallised in acetone and dried in a vacuum oven to obtain yellow crystals of 6-(4-methoxy-benzoyloxy)-hexahydro-furo[3,2-*b*]furan-3-ol (**6**). Yield: 45%. m.p.: 116°C. IR (KBr, cm^{-1}): 3451 (–OH), 2970, 2895 (CH$_3$– and –CH$_2$–), 1718 (C=O), 1607, 1510 (Ar), 1235 (C–O–C). ^{1}H-NMR (CDCl$_3$, δ, ppm): 3.26–3.34 (m, 1H, –OC<u>H</u>– in the isosorbide group); 3.75 (s, 3H, –OC<u>H</u>$_3$); 3.93–4.63 (m, 7H, –OC<u>H</u>– and –OC<u>H</u>$_2$– in the isosorbide group); 5.01–5.12 (s, 1H, –O<u>H</u>); 6.84–7.85 (m, 4H, Ar–<u>H</u>).

Compound **6** (9.1 g, 0.030 mol) and 2.0 mL dry pyridine were dissolved in 50 mL dry THF to form a solution. The THF solution of **4** (15.0 g, 0.25 mol) was added dropwise to the solution and reacted at 60°C for 38 h, then some solvent was distilled out. The mixture was cooled and poured into 600 mL of cold water. The precipitated crude product was filtered, washed with hot water and alcohol, recrystallised in THF and dried overnight under vacuum to obtain a straw yellow powder of chiral LC monomer 6-(4-methoxy-benzoyloxy)-hexahydro-furo[3,2-*b*]furan-3-yl 4'-(4-undec-10-enoyloxy-benzoyloxy)-biphenyl-4-yl adipate (**M1**). Yield: 72%. $[\alpha]_D^{20} = +37.8°$, c = 1, chloroform; m.p.: 121°C. IR (KBr, cm^{-1}): 3072, 2924, 2854 (CH$_3$–, –CH$_2$–, CH$_2$= and =CH), 1747, 1719 (C=O), 1605, 1499 (Ar). Elemental analysis: Calculated for C$_{50}$H$_{54}$O$_{13}$: C, 69.59%; H, 6.31%. Found: C, 69.43%; H, 6.23%. ^{1}H-NMR (CDCl$_3$, δ, ppm): 1.32–1.91 [m, 16H, –(C<u>H</u>$_2$)$_6$– and –(C<u>H</u>$_2$)$_2$–]; 2.05–2.20 (m, 2H, =CHC<u>H</u>$_2$–); 2.60–3.25 [m, 6H, –(CH$_2$)$_6$C<u>H</u>$_2$COO– and –OOCC<u>H</u>$_2$(CH$_2$)$_2$C<u>H</u>$_2$COO–]; 4.35–4.41 (s, 3H, –OC<u>H</u>$_3$); 5.03–5.13 (m, 2H, C<u>H</u>$_2$=CH–); 5.31–5.54 (m, 4H, –(C<u>H</u>$_2$)– in the isosorbide group); 5.83–5.90 (m, 1H, CH$_2$=C<u>H</u>–); 6.12–6.23 (m, 4H, –C<u>H</u>– in the isosorbide group); 6.94–7.95 (m, 16H, Ar–<u>H</u>).

*2.3.2 Synthesis of 4'-(4-methoxy-benzoyloxy)-biphenyl-4-yl 4-(2-undec-10-enoyloxy-ethoxy)-benzoate (**M2**)*

The synthesis routes of the nematic LC monomer **M2** are displayed in Scheme 2. Biphenyl-4, 4'-diol (93.0 g, 0.70 mol) and 8 mL pyridine were dissolved in 250 mL dry THF, which was added dropwise with THF solution of 4-methoxy-benzoyl chloride (20.5 g, 0.12 mol). The reaction mixture was stirred at 65°C for 15 h. After cooling to room temperature, the mixture was poured into 1200 mL cold water and acidified with 6 N sulfuric acid. The precipitates were isolated by filtration and dried in a vacuum oven. Recrystallisation in acetone resulted in 13.9 g white crystals of 4'-(4-methoxy-benzoyloxy)-biphenyl-4-ol (**1'**). Yield: 47%. m.p.: 209°C. IR (KBr, cm^{-1}): 3376 (–O–H), 2975, 2844 (CH$_3$– and Ar–H), 1731 (C=O), 1613, 1508 (Ar). ^{1}H-NMR (CDCl$_3$, δ, ppm): 3.75–3.92 (s, 3H, –OC<u>H</u>$_3$); 6.05–6.14 (s, 1H, –O<u>H</u>); 6.98–8.01 (m, 12H, Ar–<u>H</u>).

The intermediate **2'** was synthesised according to the reported literature (*21*). Compound **1'** (32.0 g, 0.10 mol) and 2.0 mL dry pyridine were dissolved in 200 mL dry THF to form a solution. The THF solution of

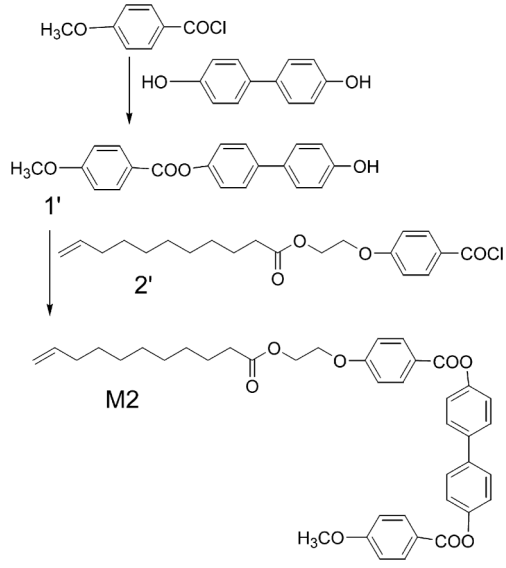

Scheme 2. Synthesis routes of 4'-(4-methoxy-benzoyloxy)-biphenyl-4-yl 4-(2-undec-10-enoyloxy-ethoxy)-benzoate (**M2**).

2' (36.6 g, 0.10 mol) was added dropwise to the solution and reacted at 60°C for 48 h, and then some solvent was distilled out. The mixture was cooled and poured into 1000 mL cold water. The precipitated crude product was filtered, washed with hot alcohol, recrystallised in THF and dried overnight under vacuum to obtain a straw yellow powder of LC monomer 4'-(4-methoxy-benzoyloxy)-biphenyl-4-yl 4-(2-undec-10-enoyloxy-ethoxy)-benzoate (**M2**). Yield: 40%. m.p.: 126°C. IR (KBr, cm^{-1}): 3066, 2927, 2853 (CH_3–, –CH_2– and Ar–H), 1745, 1725 (C=O), 1607, 1503 (Ar). Elem. Anal. Calcd. for $C_{40}H_{42}O_8$: C, 73.83%; H, 6.51%. Found: C, 73.94%; H, 6.43%. ^{1}H-NMR ($CDCl_3$, δ, ppm): 1.30–1.85 [m, 12H, –(C<u>H</u>$_2$)$_6$–]; 2.08–2.19 (m, 2H, =CHC<u>H</u>$_2$–); 2.63–3.18 [m, 2H, –$(CH_2)_6$C<u>H</u>$_2$COO–]; 4.30–4.42 (s, 3H, –OC<u>H</u>$_3$); 5.05–5.12 (m, 2H, C<u>H</u>$_2$=CH–); 5.60–5.78 (m, 4H, –OC<u>H</u>$_2$C<u>H</u>$_2$O–); 5.80–5.87 (m, 1H, CH_2=C<u>H</u>–); 6.98–7.89 (m, 16H, Ar–<u>H</u>).

2.3.3 *Synthesis of the polymers*

For synthesis of polymers **P1**–**P6**, the same method was adopted. The polymerisation experiments are summarised in Table 1. The synthesis of polymer **P4** was given as an example. Chiral LC monomer **M1** (1.05 mmol) was dissolved in 50 mL of dry, fresh distilled toluene. To the stirred solution, LC monomer **M2** (0.70 mmol), PMHS (0.25 mmol) and a Pt catalyst were added and heated under nitrogen and anhydrous conditions at 65°C for 40 h. Then the mixture was cooled and poured into methanol. After filtration, the product was dried at 80°C for 4 h under vacuum to obtain a polymer in the yield of 90%.

3. Results and discussion

3.1 *Syntheses*

For the monomers, the structures of **M1** and **M2** were characterised using IR and ^{1}H-NMR spectra, which was in good agreement with the prediction. The spectra of **M1** and **M2** suggest that the purity is high and this was confirmed by elementary analysis.

Polymers **P1**–**P6** were prepared by a one-step hydrosilylation reaction between Si–H groups of PMHS and olefinic C=C of **M1** and **M2** in toluene, with hexachloroplatinic acid as a catalyst. The obtained polymers were soluble in toluene, xylene, THF, chloroform and so forth. Their structures were characterised by use of IR and ^{1}H-NMR spectra. Polymer **P4** contains the representative features for all of the polymers. Figure 1 displays the FTIR spectra of **P4**. Their characteristic absorption bands are as follows: 2945–2847 cm^{-1} (C–H stretching), 1746–1715 cm^{-1} (C=O stretching in different kinds of ester modes), 1608, 1510 cm^{-1} (aromatic stretching) 1192–1080 cm^{-1} (Si–O–Si stretching). In Figure 1, the absorptions for the Si–CH_3 bonds were at 1265 and 843 cm^{-1}. The disappearance of most of PMHS Si–H stretching at 2160 cm^{-1} and the olefinic C=C stretching band at 1635 cm^{-1} indicates successful incorporation of the monomers into the polysiloxane chains. In addition, the ester C=O absorption bands on monomers **M1** and **M2** and the characteristic Si–O–Si broad stretching bands on PMHS still existed in the polymers. For the LC polysiloxanes, it is necessary to know the polymer composition and molecular weights. Therefore, we have made the NMR analyses of the polymers, taking into consideration the solubility in chloroform. The ^{1}H-NMR spectrum of **P4** and its chemical structure are shown in Figure 2. The

Table 1. Polymerisation, polymer composition, thermal properties and specific rotation of the polymers.

	Feed	**M2/M1** ratio[a]		T_d[c]	DSC[d]			
Sample	PMHS/**M1**/**M2** (mmol)	(%)	M_n[b]	(°C)	T_g (°C)	$T_{S\text{-}Ch}/\Delta H$ (°C)/J·g^{-1}	T_i (°C)	$[\alpha]_D^{20}$[e]
P1	0.25/1.75/0.00	0	5900	329	–9.9	132.5/1.63	176.1	+9.8
P2	0.25/1.57/0.18	11	5700	321	–9.8	130.1/0.94	175.3	+8.1
P3	0.25/1.40/0.35	24	5600	327	–8.0	–	169.4	+6.9
P4	0.25/1.05/0.70	65	5400	319	–9.9	–	174.6	+5.2
P5	0.25/0.70/1.05	146	5200	305	–7.7	–	173.2	+3.7
P6	0.25/0.35/1.40	396	4800	317	–9.2	–	174.8	+2.5

[a]Comparison of the integration of the –C<u>H</u>– signals of the isosorbide group (corresponding to the **M1** component) to those of the –OC<u>H</u>$_2$C<u>H</u>$_2$O–signals (corresponding to the **M2** component).
[b]Calculated according to both the **M2/M1** ratio and the substitution degree.
[c]Temperature at which 5% weight loss occurred.
[d]Phase transition and enthalpy changes on the second heating.
[e]Specific rotation of polymers, 0.1 g in 10 mL $CHCl_3$.

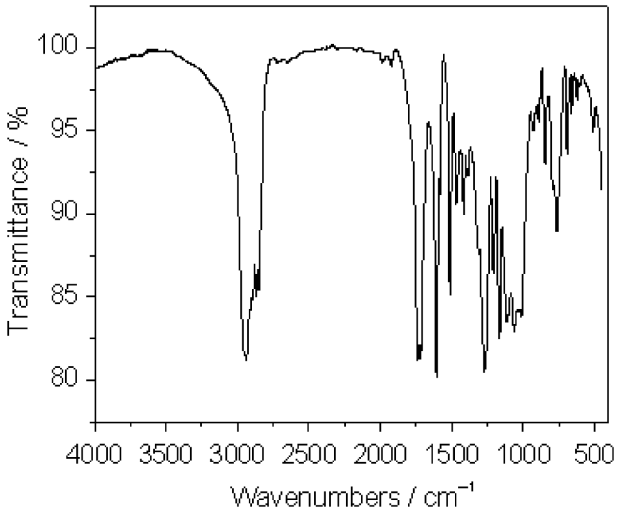

Figure 1. FTIR spectrum of polymer **P4**.

characteristic ^{1}H-NMR peaks are as follows: 0.15–0.62 (Si–C<u>H</u>$_3$ and Si–C<u>H</u>$_2$–, ***a*** and ***b***); 1.29–2.65 (–C<u>H</u>$_2$–, ***c***); 2.60–3.25 [m, 6H, –(CH$_2$)$_6$C<u>H</u>$_2$COO– and –OOCC<u>H</u>$_2$(CH$_2$)$_2$C<u>H</u>$_2$COO–, ***d***]; 4.15–4.40 (–OC<u>H</u>$_3$, ***e***); 5.19–5.31 (–C<u>H</u>$_2$– in isosorbide group, ***f***); 5.43–5.62 (–OC<u>H</u>$_2$C<u>H</u>$_2$O–, ***g***); 6.15–6.24 (–C<u>H</u>– in isosorbide group, ***h***); 6.97–7.94 ppm (Ar–<u>H</u>, ***i***). On the one hand, no signals characteristic of terminal olefinic moiety in the monomers appeared in the ^{1}H-NMR spectra, suggesting excess monomers were eliminated from the polymers. On the other hand, the δ value of –SiH– was shown to be near 4.68 ppm in the ^{1}H-NMR spectrum of PMHS, but there was no peak near 4.68 ppm for all of the polymers. For PMHS, the substitution degree can be determined by comparison of the integration of the Si–H signals to those of the Si-methyl groups. Disappearance of the peak near 4.68 ppm indicated that all of the Si–H bonds in PMHS were substituted via the hydrosilylation action, and the monomers were connected to the polysiloxane chains. In order to find the polymer composition, the **M1/M2** ratio can be determined by comparison of the integration of the –C<u>H</u>– signals of the isosorbide group (**M1** component) to those of the –OC<u>H</u>$_2$C<u>H</u>$_2$O– signals (**M2** component) in the polymer systems. Furthermore, the molecular weights M_n can be calculated according to both the **M2/M1** ratio and the substitution degree. The polymer composition, substitution degree and molecular weights determined by ^{1}H-NMR analyses of the polymers are listed in Table 1. It was shown that the molecular weights decreased slightly with the increase of the **M2** component.

3.2 *Optical rotation analysis*

The optical properties of chiral LCPs result from chiral molecules that induce a twist in the director of the adjacent molecules, thereby forming a super molecular helical structure. Therefore, it is interesting to study the optical rotation (α) of the chiral LCPs.

Although the chiral monomer **M1** bearing isosorbide segments showed significantly higher specific rotations ($[\alpha]_D^{20} = +37.8°$), the specific rotations of the chiral LCPs displayed low positive values (as shown in Table 1), suggesting cleavage of the

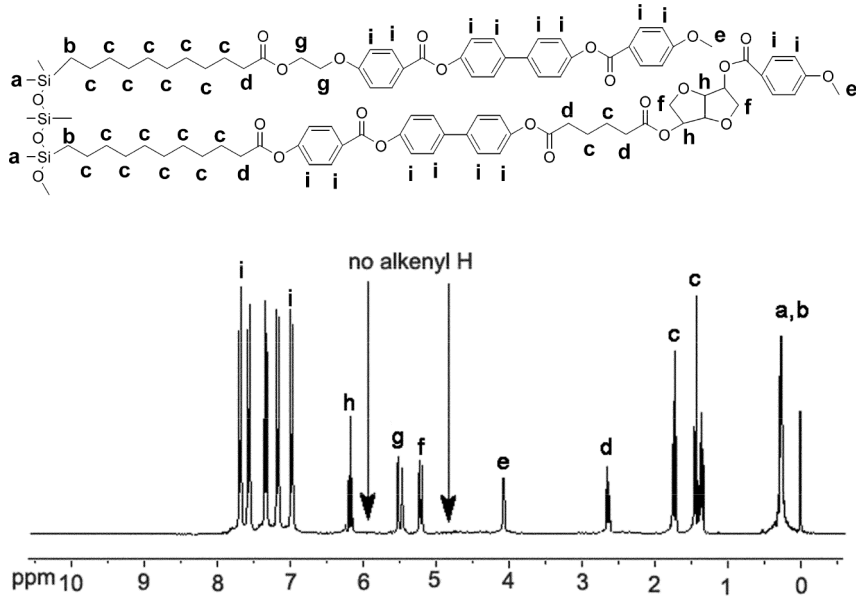

Figure 2. The chemical structure and ^{1}H-NMR spectrum of **P4**.

double bond, and the binding of two monomers to the polysiloxane main chains seemed to significantly affect the chirality of the compounds. For the polymers, the specific rotation value decreased with the decrease of chiral groups in the polymer systems.

3.3 Liquid crystalline behaviours of the monomers

Differential scanning calorimetry (DSC) curves of chiral LC monomer 6-(4-methoxy-benzoyloxy)-hexahydro-furo[3,2-*b*]furan-3-yl 4'-(4-undec-10-enoyloxy-benzoyloxy)-biphenyl-4-yl adipate (**M1**) showed a melting transition at 121.4°C (corresponding enthalpy changes ΔH = 26.80 $J \cdot g^{-1}$) and a Ch–isotropic phase transition at 279.6°C (ΔH = 1.62 $J \cdot g^{-1}$) on heating and displayed an isotropic–Ch phase transition at 259.5°C (ΔH = 2.37 $J \cdot g^{-1}$) and a crystallisation process at 99.9°C (ΔH = 18.98 $J \cdot g^{-1}$) on cooling, as shown in Figure 3(a). The DSC heating curves of 4'-(4-methoxy-benzoyloxy)-biphenyl-4-yl 4-(2-undec-10-enoyloxy-ethoxy)-benzoate (**M2**) contained two endotherms of the phase transition, which represent a melting transition at 126.3°C (ΔH = 10.16 $J \cdot g^{-1}$) and a nematic-to-isotropic phase transition at 260.9°C. (ΔH = 3.56 $J \cdot g^{-1}$). On cooling scans of **M2**, there was an isotropic–nematic phase transition at 257.6°C (ΔH = 2.89 $J \cdot g^{-1}$) and the crystallisation temperature appeared at 119.1°C (ΔH = 2.65 $J \cdot g^{-1}$), as shown in Figure 3(b).

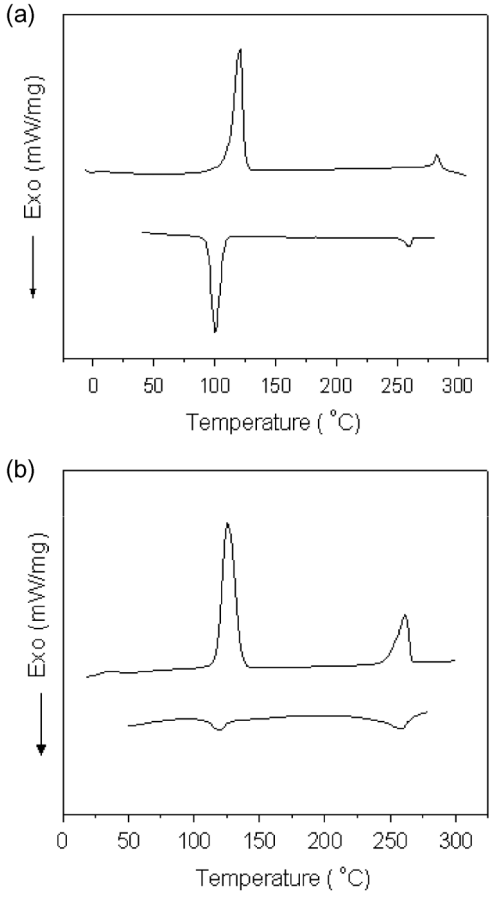

Figure 3. DSC thermograms of the monomers for (a) **M1** and (b) **M2** on the second heating and the first cooling.

The optical textures of the monomers were studied by means of polarised optical microscopy (POM) with a hot stage (see Figure 4). The POM results showed that **M1** exhibited an enantiotropic Ch phase, and **M2** exhibited nematic phases on the heating and cooling cycles. When **M1** was heated to 269°C, the typical Ch oily streak texture appeared, as shown in Figure 4(a). When **M2** was heated to 126°C, the sample began to melt, a nematic schlieren texture appeared and mesomorphic behaviour disappeared at 260°C. When the isotropic state was cooled, the nematic droplet and schlieren texture appeared and it crystallised at 119°C. The optical textures of **M2** are shown in Figure 4(b).

3.4 Mesomorphic properties of the polymers

The phase-transition temperatures and corresponding enthalpy changes to polymers **P1**–**P6**, which were obtained on the second heating, are summarised in Table 1. All phase transitions were reversible and did not change on repeated heating and cooling cycles. The phase-transition temperatures determined by

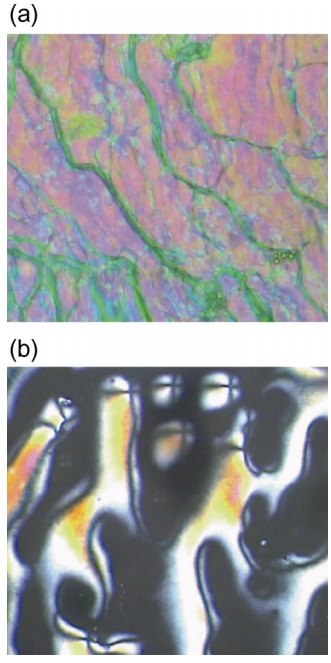

Figure 4. Optical texture of the monomers (200×): (a) oily streak texture of **M1** at heating to 269°C; (b) schlieren texture of **M2** at heating to 211°C.

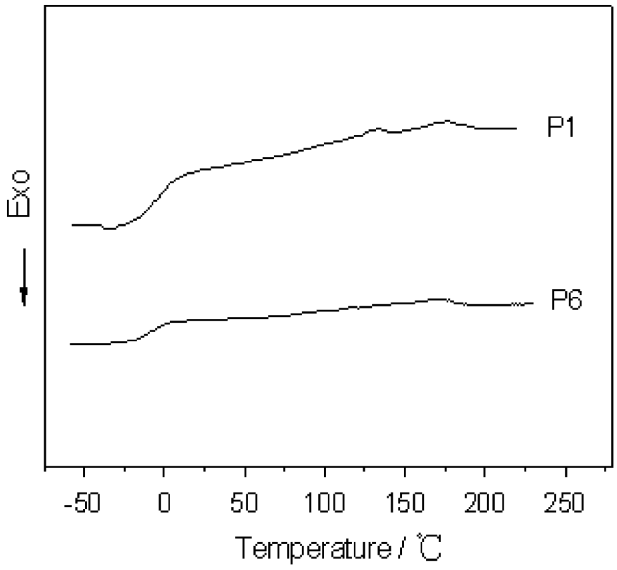

Figure 5. DSC thermograms of representative polymers **P1** and **P6** on the second heating.

DSC were consistent with POM observation results. DSC thermograms of representative polymers **P1** and **P6** are shown in Figure 5.

DSC thermograms of **P1** and **P2** showed a glass transition, a smectic–Ch transition and a Ch–isotropic transition on heating cycles. Polymers **P3–P6** displayed only a Ch phase and the smectic phase did not appear on the heating and cooling cycles. The glass transition temperature (T_g) of all polymers did not change greatly with increased **M2** in the polymer systems, while the isotropic temperature (T_i) decreased slightly on the heating cycles. The polymer backbone, the rigidity of the mesogenic units and the length of the flexible spacer would influence the mesophase behaviours of the polymers. Because of the same polymer backbone and the similar length of the flexible spacer in **M1** and **M2**, all of the polymers displayed a similar T_g. However, the difference between the mesogens in **M1** and **M2** leads to a decrease of T_i.

Thermogravimetric analysis (TGA) results of the polymers showed that the temperatures at which 5% weight loss occurred (T_d) were >300°C (the data are listed in Table 1), indicating that the synthesised polymers and LC phase have a high thermal stability. Some representative TGA thermograms of the polymers are displayed in Figure 6.

The mesomorphic properties of the polymers were also studied by means of POM with a hot stage. All the polymers displayed typical Ch oily streak textures, which were characteristic textures of Ch LC state. For **P1** and **P2**, when they were heated from room temperature, the optical textures varied greatly. However **P3**–**P6** did not change greatly when they

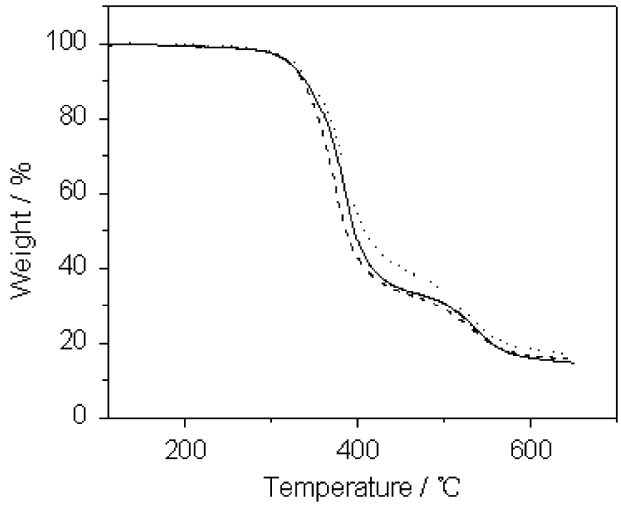

Figure 6. TGA thermograms of the representative polymers (**P2**, **P4** and **P6**) (from the top down).

were heated. When the sample **P1** was heated above room temperature, the viewing field of the polarizing microscope became bright and LC textures appeared. The textures became obvious as the sample was heated continuously and a focal conic texture appeared at heating to 63°C (see Figure 7(a)). When it was heated above 132°C, the sample flowed rapidly and formed an oily streak texture, as shown in Figure 7(b).

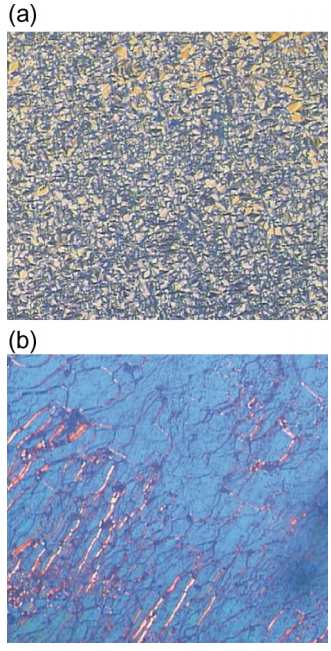

Figure 7. Optical texture of representative polymer **P1** (200×): (a) focal conic texture on heating to 63°C; (b) oily streak texture on heating to 175°C.

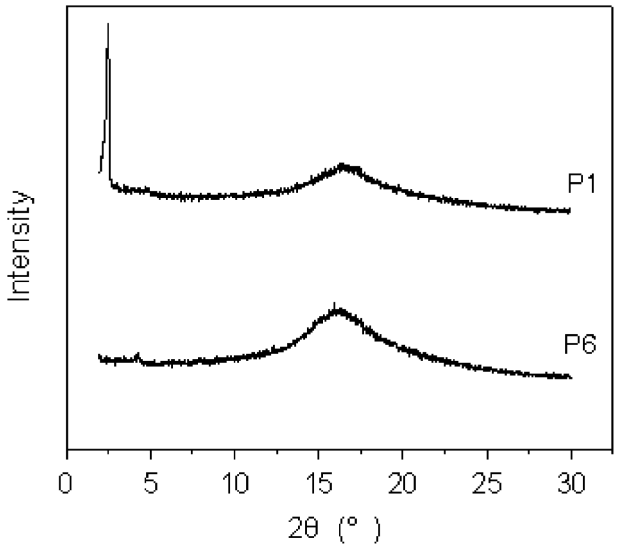

Figure 8. XRD diagrams of representative polymers **P1** and **P6**.

The smectic phases of **P1** and **P2** and the Ch phases of **P3**–**P6** were also determined by use of X-ray measurements. Figure 8 shows representative XRD curves of samples of **P1** and **P6**. For **P1** and **P2**, strong small angle reflections were observed at $2\theta \approx 2.7°$ corresponding to *d*-spacing of $d = 37.7$ Å. The strong peaks at low angles have been assigned to the layer spacing of the smectic mesophase. In addition, a broad peak appeared at $2\theta = 16.4$–$17.2°$, rather than at $2\theta \approx 20°$, suggesting a chiral helix structure between two neighbouring LC molecules within the layers of the mesophase. In general, a sharp and strong peak at a low angle ($1° < 2\theta < 4°$) in small-angle X-ray scattering (SAXS) curves and a strong, broad peak associated with lateral packing at $2\theta \approx 20°$ can be observed in wide-angle X-ray diffraction (WAXD) curves for a normal smectic polymer structure. For nematic and Ch structures of polymer systems, no strong peak appears in the SAXS curves. However, a broad peak at $2\theta \approx 20°$ and $2\theta \approx 17°$ was observed in the WAXD curves of the nematic and Ch polymers, respectively (*21*, *22*). Therefore, broad diffraction angles appearing at a lesser angle than those of nematic structures in WAXD is a very important characteristic for judging a Ch structure. It suggests that the average distance between two neighbouring LC molecules within the layers of the mesophase become broad due to the helix structure of Ch LCPs. Therefore, the chiral smectic mesophase structure of **P1** and **P2** was confirmed by the XRD results. For polymers **P3**–**P6**, there is no strong peak at $2\theta \approx 2.7°$, but a broad peak at $2\theta \approx 17°$ was observed in the WAXD curves, suggesting that they are Ch polymers.

For all of the LCPs, the chiral groups in the polymer systems lead to the appearance of a Ch phase. Because **P1** and **P2** contain the majority of the chiral LC monomer **M1**, regular structures in the polymer systems lead to the appearance of a smectic phase. With increased non-chiral groups of **M2** in the polymers **P3**–**P6**, the regular structures were destroyed because of the different chemical structures between **M1** and **M2**, resulting in the disappearance of the smectic arrangement.

4. Conclusions

A series of LC polysiloxanes were synthesised with a Ch monomer 6-(4-methoxy-benzoyloxy)-hexahydro-furo[3,2-*b*]furan-3-yl 4'-(4-undec-10-enoyloxy-benzoyloxy)-biphenyl-4-yl adipate and a nematic LC monomer 4'-(4-methoxy-benzoyloxy)-biphenyl-4-yl 4-(2-undec-10-enoyloxy-ethoxy)-benzoate. The chemical structures and LC properties of the monomers and polymers were characterised by various experimental techniques including FTIR, ^{1}H-NMR, EA, DSC, POM and XRD. Polymers **P1** and **P2**, which contain the majority of the chiral LC monomers **M1**, showed smectic and Ch mesophases. The other polymers bearing two kinds of LC monomers displayed only the Ch mesophase. All of the chiral LCPs showed LC properties with very wide mesophase temperature ranges.

The polymers bearing the majority of the one chiral LC monomer showed a smectic phase resulting from regular structures in the polymer systems. With the increase of another nematic LC monomer in the polymers, the regular structures were destroyed because of the different chemical structures between the two kinds of LC monomers, leading to the disappearance of the smectic arrangement. For all of the chiral LCPs, the chiral groups in the LCP systems lead to the appearance of a Ch phase.

Acknowledgments

The authors are grateful to the National Natural Science Fundamental Committee of China and the Science and Technology Department of Liaoning Province for financial support.

References

(1) Walba, D.M.; Yang, H.; Shoemaker, R.K.; Keller, P.; Shao, R.; Coleman, D.A.; Jones, C.D.; Nakata, M.; Clark, N.A. *Chem. Mater.* **2006**, *18*, 4576–4584.
(2) Li, C.Y.; Ge, J.J.; Bai, F.; Zhang, J.Z.; Calhoun, B.H.; Chien, L.C.; Harris, F.W.; Lotz, B.; Cheng, S.Z.D. *Polymer* **2000**, *41*, 8953–8960.
(3) Meng, F.B.; Lian, J.; Chen, H.B.; Gao, Y.M.; Zhang, B.Y. *High Perform. Polym.* **2009**, *21*, 64–78.
(4) Hwang, J.C.; Shu, M.C.; Lin, C.P. *Macromol. Chem. Phys.* **1999**, *200*, 2250–2256.

(5) Meng, F.; Lian, J.; Zhang, B.; Sun, Y. *Eur. Polym. J.* **2008**, *44*, 504–513.
(6) Shibaev, V.; Bobrovsky, A.; Boiko, N. *Prog. Polym. Sci.* **2003**, *28*, 729–836.
(7) Meng, F.B.; Gao, Y.M.; Zhang, B.Y.; Xu, X.X. *J. Macromol. Sci. Part A* **2008**, *45*, 186–194.
(8) Sun, S.J.; Schwarz, G.; Kricheldorf, H.R.; Chang, T.C. *J. Polym. Sci. Part A: Polym. Chem.* **1999**, *37*, 1125–1133.
(9) Meng, F.B.; Zhang, B.Y.; Xiao, W.Q.; Hu, T.X. *J. Appl. Polym. Sci.* **2005**, *96*, 625–631.
(10) Kricheldorf, H.R.; Krawinkel, T. *Macromol. Chem. Phys.* **1998**, *199*, 783–790.
(11) Kricheldorf, H.R.; Sun, S.J.; Chen, C.P.; Chang, T.C. *J. Polym. Sci. Part A: Polym. Chem.* **1997**, *35*, 1611–1619.
(12) Schwarz, G.; Kricheldorf, H.R. *J. Polym. Sci. Part A: Polym. Chem.* **1996**, *34*, 603–611.
(13) Hsiue, G.H.; Chen, J.H. *Macromolecules* **1995**, *28*, 4366–4376.
(14) Hsu, L.L.; Chang, T.C.; Tsai, W.L.; Lee, C. *J. Polym. Sci. Part A: Polym. Chem.* **1997**, *35*, 2843–2855.
(15) Hsiue, G.H.; Lee, R.H.; Jeng, R.J.; Chang, C.S. *J. Polym. Sci. Part B: Polym. Phys.* **1996**, *34*, 555–563.
(16) Hiraoka, K.; Stein, P.; Finkelmann, H. *Macromol. Chem. Phys.* **2004**, *205*, 48–54.
(17) Sapich, B.; Stumpe, J.; Kricheldorf, H.R.; Schonhals, A. *Macromolecules* **2001**, *34*, 5694–5701.
(18) Yue, Z.; Cowie, J.M.G. *Macromolecules* **2002**, *35*, 6572–6577.
(19) Li, C.Y.; Cheng, S.Z.D.; Ge, J.J.; Bai, F.; Zhang, J.Z.; Mann, I.K.; Chien, L.; Harris, F.W.; Lotz, B. *J. Am. Chem. Soc.* **2000**, *122*, 72–79.
(20) Meng, F.B.; Cui, Y.; Chen, H.B.; Zhang, B.Y.; Jia, C. *Polymer* **2009**, *50*, 1187–1196.
(21) Hu, J.S.; Zhang, B.Y.; Zhou, A.J.; Dong, Y.L.; Zhao, Z.X. *J. Polym. Sci. Part A: Polym. Chem.* **2005**, *43*, 3315–3323.
(22) Meng, F.B.; Zhang, B.Y.; Li, Q.Y. *Polym. J.* **2005**, *37*, 277–283.